Molecular Understanding of Osmosis in Semipermeable Membranes

A. V. Raghunathan and N. R. Aluru*

Department of Mechanical Science and Engineering, Beckman Institute for Advanced Science and Technology, University of Illinois at Urbana-Champaign, Urbana, Illinois 61801, USA

(Received 12 December 2005; published 10 July 2006)

We investigate single-file osmosis of water through a semipermeable membrane with an uncharged, a positively and a negatively charged nanopore. Molecular dynamics simulations indicate that the osmotic flux through a negatively charged pore (J_-) is higher compared to the osmotic flux in a positively charged pore (J_+) followed by the osmotic flux in the uncharged pore (J_0), i.e., $J_- > J_+ > J_0$. The molecular mechanisms governing osmosis, steady state osmosis, and the observed osmotic flux dependence on the nanopore charge are explained by computing all the molecular interactions involved and identifying the molecular interactions that play an important role during and after osmosis. This study helps in a fundamental understanding of osmosis and in the design of advanced nanoporous membranes for various applications of osmosis.

DOI: 10.1103/PhysRevLett.97.024501 PACS numbers: 82.39.Wj, 47.56.+r, 47.61.−k

In all living matter, osmosis is a primary passive mode of ''pumping'' water, which is an essential ingredient to life. Osmosis is a complex phenomenon in which a solvent is driven by its free energy gradient through a semipermeable membrane towards a solute-rich reservoir. Osmosis has been studied extensively because of its impact in a variety of areas, including separation of metal ions from water using reverse osmosis membranes. Osmosis is also pervasive in biological systems, where the distribution of nutrients and the release of metabolic waste products is controlled by osmosis [1]. Aquaporin, a water channel present in cell membranes, depends on water in its local environment and utilizes the osmotic pressure for many critical functions. In humans, the method by which nitrogenous waste is removed from kidneys is based on osmosis, and the physiology of most aquatic organisms is dominated by methods of maintaining some form of osmoregularity in relation to the changing environment. There have been several molecular dynamics (MD) studies of hard-sphere Lennard-Jones (LJ) atoms (see, e.g., [2]) to understand osmosis, and, more recently, these studies have been extended to water transport driven by an osmotic salt gradient through carbon nanotube arrays [3]. In spite of the vast literature on osmosis, several aspects of the osmotic phenomenon remain unanswered including a molecular understanding (which molecular interactions initiate osmosis, what molecular interactions are significant at steady state, etc.) of osmosis and the dependence of osmosis on the charge of the membrane. In this Letter, using molecular dynamics simulations, we first compute the osmotic flux through uncharged, positively charged, and negatively charged semipermeable membranes. Our results indicate that the osmotic flux through a negatively charged membrane is highest, followed by positively charged and uncharged membranes. Next, we try to provide a fundamental understanding of osmosis in uncharged and charged semipermeable membranes. Specifically, we identify the key intermolecular forces that initiate osmosis in uncharged and charged membranes and explain the significance of various intermolecular forces as the system evolves to a steady state.

Figure 1 shows a snapshot of the MD simulation system. The system consists of two square membranes (3.3 nm long in the x and y directions and 1.5 nm thick in the z direction) separating two KCl solutions of different concentrations. The membrane atoms are located in a face centered cubic fashion in the xy plane. Each membrane consists of a semipermeable pore (only water can go through the pore and ions do not go through the pore) of diameter 0.9 nm at the center of the membrane. Figure 1 also shows the dimensions of the solution chambers connecting each membrane. Two membranes are connected back to back as shown in Fig. 1, and periodic boundary conditions are applied to the system in all three directions [2]. For charged pore simulations, the pore wall is assigned discrete charges on the atoms to produce a net charge density of ± 0.12 C/m^2. The membrane and the pore wall atoms are modeled as LJ atoms with parameters for carbon [4], and the atoms are frozen to their original lattice positions. A simple point charge-extended model is used for water, while ions are modeled as charged LJ atoms [5,6].

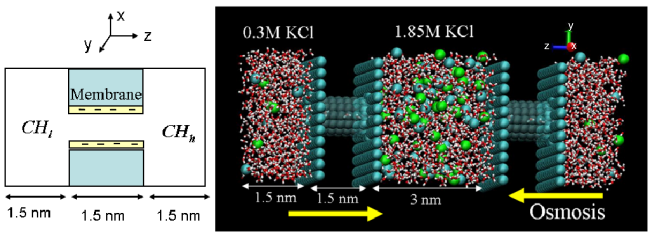

FIG. 1 (color online). A schematic (left) and a snapshot (right) of the MD simulation system for osmosis. The high solute concentration chamber is denoted by CH_h, and the low solute concentration chamber is denoted by CH_l.

MD simulations were performed using GROMACS 3.1.4 [7] in an *NVT* ensemble. A Berendsen thermostat was used to maintain the temperature of the fluid at 300 K. The electrostatic interactions were computed by using the particle mesh Ewald method [8]. The LJ cutoff distance and the real space cutoff distance for electrostatic calculations was 1 nm. The low and high solute chambers were initially filled with a KCl solution of 0.3 and 1.85 M concentrations, respectively. The number of ions in the two chambers does not change during the simulation, as the membrane pores are permeable only to water. The hydrostatic pressure of the two chambers was calculated from the force exerted on the membrane wall atoms. Water was allowed to enter the pore during a 1 ns equilibration run. Thereafter, the simulation was run a further 200 ps to ensure that the pressure in the two chambers is the same (≈ 40 bar). This prevents any pressure driven flow through the pore at the start of osmosis. Two different initially equilibrated configurations were simulated in MD for 4 ns while keeping the initial number of water and solute molecules the same in both the simulations. The trajectory was saved every 0.1 ps, and the calculation of the mean force for postprocessing analysis was carried out on the fly during the simulation. Simulation results described below are obtained after averaging over the two production runs of 4 ns each.

Three simulations with pore wall surface charge densities of 0, 0.12, and -0.12 C/m^2 were performed. The osmotic flux variation in all the three cases was calculated. The number of water molecules accumulated in the high solute chamber (CH_h) of 1.85 M KCl and the decrease in the number of water molecules in the low solute chamber (CH_l) of 0.3 M KCl with time are shown in Fig. 2. The osmotic flux is initially dominant leading to an increase or decrease in the number of water molecules in CH_h and CH_l, respectively. As shown in Fig. 2, the water occupancy in each chamber saturates after about 2 ns, indicating that a steady state has been reached. The number of water molecules accumulated in CH_h (or the decrease in the number of water molecules in CH_l) is dependent on the membrane polarity. Specifically, the osmotic flux in the negatively charged pore (J_-) is higher compared to the osmotic flux in the positively charged pore (J_+), and the osmotic flux in the uncharged pore (J_0) is the lowest, i.e., $J_- > J_+ > J_0$.

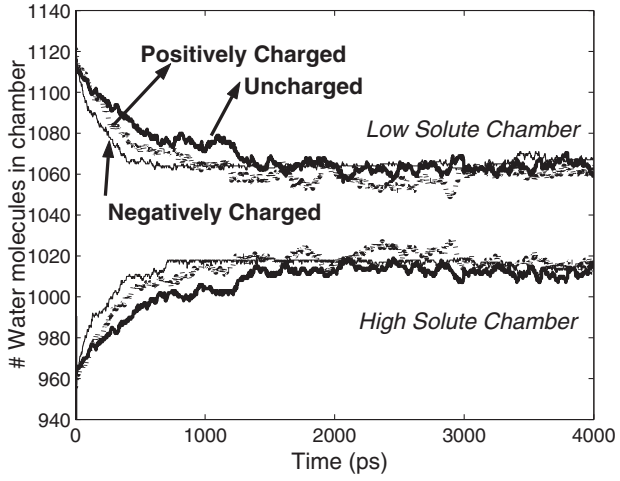

FIG. 2. Variation of the water occupancy in the two chambers with time for the three membrane pore polarities of 0, 0.12, and -0.12 C/m^2. Low solute chamber drains, while the high solute chamber accumulates water molecules.

To understand these results, we computed the total mean force [9] acting on a water molecule in the axial direction (z direction) as an average over time along the center line of the pore from the summation of the LJ ($12-6$) interaction and the electrostatic interaction, which is computed using the Ewald summation [8]. Figure 3 shows the mean force on a water molecule for the uncharged pore. A positive mean force moves the water molecule in the direction of CH_l to CH_h, and a negative mean force moves the water molecule in the direction of CH_h to CH_l. We note that the mean force due to ion-water interactions is asymmetric at the ends of the pore region; i.e., the mean force is higher near the pore mouth connected to CH_h compared to the mean force near the pore mouth connected to CH_l. The tendency for the ions in the reservoir to ''pull'' the water molecules towards them to maintain their hydration shell is dominant in CH_h compared to CH_l. Thus, a higher mean force on water is observed near the pore mouth connected to CH_h. The asymmetry in the mean force on water due to ion-water interactions causes water to move from CH_l to CH_h. The asymmetry in the mean force on water due to the water-water and wall-water interactions is not as significant [see Fig. 3 (inset)]. From this discussion, we can conclude that osmosis in uncharged pores is primarily initiated by ion-water interactions.

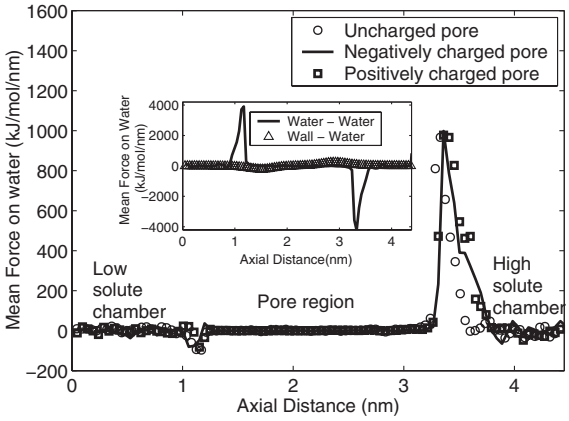

FIG. 3. Mean force on water (averaged over 1.5 ns) due to ion-water interactions in the positive, negative, and uncharged pores. Inset: Mean force on a water molecule (averaged over 1.5 ns) in the axial direction along the center line of the uncharged pore due to water-water and wall-water interactions. A positive mean force means that water is driven from the low solute chamber to the high solute chamber and vice versa. The first 1.5 ns represents about 75% of the osmosis duration.

When the pores are charged, in addition to the ion-water asymmetry (see Fig. 3) near the pore mouth regions, the mean force on the water molecules due to the water-wall electrostatic interactions is also found to be asymmetric as shown in Fig. 4. The asymmetry in other interactions (e.g., water-water) is negligible, though some of these interactions can be different in charged pores when compared to the uncharged pores. The effect of ion-water asymmetry on osmosis in charged pores is similar to that of in an uncharged pore. In addition to ion-water asymmetry, Fig. 4 indicates that the net mean force on a water molecule in the axial direction due to water-wall electrostatic interactions is higher near the pore mouth connected to CH_l compared to the mean force near the pore mouth connected to CH_h. The positive mean force near the pore mouth connected to CH_l moves the water molecules from CH_l to CH_h. Since the positive mean force is much higher compared to the negative mean force, the net water movement (osmosis) is from the low solute chamber to the high solute chamber. From the above discussion, in the case of charged pores, we can infer that the osmosis is primarily caused due to the asymmetry in ion-water and water-wall electrostatic interactions, while in the case of uncharged pores the osmosis is primarily due to the asymmetry in the ion-water interactions. As a result, the osmotic flux in positively and negatively charged pores is found to be higher compared to the osmotic flux in the uncharged pore.

The flux in the negatively charged pore (J_-) is higher compared to the flux in the positively charged pore (J_+). This can be explained from Fig. 4 by noting that the mean force on water (near the pore mouth connected to CH_l) due to water-wall electrostatic interactions is higher in the negatively charged pore compared to the positively charged pore. Note that the mean force near the pore mouth connected to CH_h in both positively and negatively charged pores is similar, so the asymmetry is higher in the case of a negatively charged pore. The higher mean force near the pore mouth connected to CH_l in the negative pore can be explained by comparing the dipole orientation of water in the two charged pores. The inset in Fig. 4 shows the time averaged dipole orientation of water with respect to the z axis along the center line of the pore. The dipole orientation is calculated by using the angle made by the angle bisector of H-O-H with the positive z axis. A positive $\langle\cos(\theta)\rangle$ value implies that the water enters the pore in a single file with the hydrogen atoms first. The water orientation during osmosis through the pore is opposite in the positive and negative pores. In the negative pore, water molecules enter with hydrogen atoms first, while the oxygen atoms enter first in the positively charged pore. Since the LJ interactions of the hydrogen atoms are negligible, in the negatively charged pore they tend to go closer to the pore wall, giving rise to a higher electrostatic interaction with the wall. Thus, the water molecules in the negative pore experience a higher mean force due to wall-water electrostatic interaction compared to a positively charged pore.

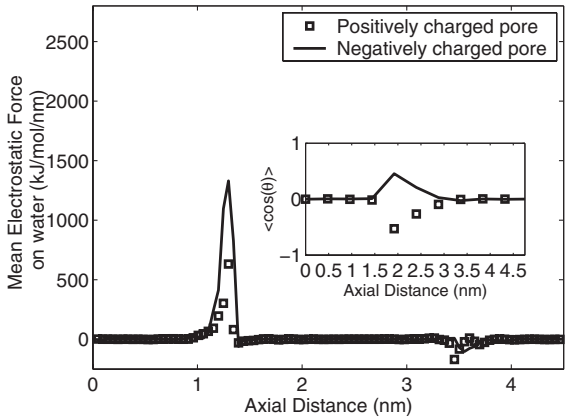

FIG. 4. Mean force on a water molecule (averaged over 1.5 ns) in the axial direction along the center line of the pore due to water-wall electrostatic interactions. Inset: Dipole orientation of water (averaged over 1.5 ns) in the positively and negatively charged pores along the center line axis. θ is the angle between the H-O-H dipole and the positive z axis.

The osmotic flux through the nanopore can also be understood qualitatively by computing the probability of the water chain to be broken in the pore. The probability of the single-file water chain being broken in the pore during osmosis was calculated for the uncharged and charged pores by dividing the number of times the water chain is broken during the 1.5 ns simulation time with the total number of steps at which statistics were collected (every 2.5 ps). The probability for the water chain to be broken is highest in the uncharged pore and lowest in the negative pore, as shown in Table I. A lower probability for the single-file water chain to be broken also suggests a higher osmotic flux.

During osmosis, the total mean force on water molecules is unbalanced across the pore. As time progresses, an increase in the number of water molecules in the CH_h chamber leads to a more negative mean force on the water molecules in the pore mouth region connected to CH_h. A steady state is reached when the positive mean force acting on the water molecules is balanced by the negative mean force. In the case of an uncharged pore, we observe that (see Fig. 5) during steady state the net mean force on water due to water-water interactions (about -700 KJ/mol/nm) is balanced by the net mean force on water due to ion-water interactions (about 700 KJ/mol/nm). Note that at steady state the ion-water asymmetry across the pore is lower

TABLE I. Probability for the water chain to be broken in the pore (averaged over 1.5 ns).

Uncharged	Positively charged ($\sigma = 0.12$ C/m^2)	Negatively charged ($\sigma = -0.12$ C/m^2)
0.8	0.36	0.056

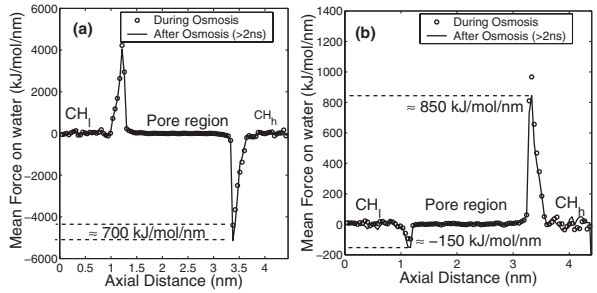

FIG. 5. Mean force on water in the axial direction along the center line of the pore due to (a) water-water and (b) ion-water interactions, during (averaged over 1.5 ns) and after (averaged over 2–4 ns) osmosis in the uncharged pore. At steady state, the asymmetric ion-water mean force is counterbalanced by the asymmetric water-water mean force.

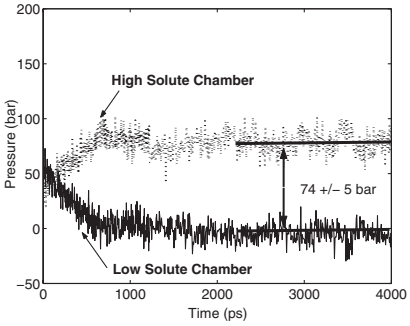

FIG. 6. Hydrostatic pressure variation on the chamber walls (CH_l and CH_h) over time. Pressure increases in CH_h during osmosis and then saturates to a constant pressure difference (between CH_h and CH_l) of 74 bar.

compared to the ion-water asymmetry during osmosis and the asymmetry in other interactions (e.g., water-wall interactions) across the pore is still negligible at steady state. In the case of charged pores, we observe that during steady state the net negative mean force on water due to water-water interactions is balanced by the net positive mean force on water due to wall-water electrostatic and ion-water interactions. The above study, when repeated for a larger semipermeble pore of 1.2 nm diameter, yielded similar observations of the osmotic flux variation, indicating that the mechanism of water transport does not change as long as the pores are strictly semipermeable.

Steady state osmosis can be described by using the Van't Hoff equation $\Delta\Pi = RT\Delta C$, where R is the gas constant, T is the absolute temperature, and ΔC is the average solute concentration difference between the two chambers. By substituting the corresponding solute concentrations into the Van't Hoff equation, the pressure difference between the two chambers is estimated to be 70 bar. We also computed the hydrostatic pressure in the two chambers using MD, and Fig. 6 shows the variation of the hydrostatic pressure with time in both chambers. At steady state, the pressure difference between the two chambers is about 74 bar, which matches reasonably well with the prediction from the Van't Hoff equation. From a molecular point of view, our results seem to suggest that at steady state the asymmetry in water-water interactions is the primary contribution to the pressure difference between the two chambers.

In summary, for single-file water transport through semipermeable nanopores, using MD simulations, we found that the osmotic flux in charged pores is higher compared to the osmotic flux in an uncharged pore. While ion-water interactions initiate osmosis in uncharged pores, both ion-water and wall-water electrostatic interactions initiate osmosis in the charged pores. During steady state, the mean force due to water-water asymmetry is primarily balanced by the mean force due to the ion-water (and wall-water in the case of charged pores) asymmetry. In the case of charged pores, water orientation near the mouth of a nanopore is found to be important and is shown to influence the osmotic flux.

This research was supported by NSF under Grant No. 0120978, No. 0523435, and No. 0328162 and by NIH under Grant No. PHS 2 PN2 EY016570B.

*Corresponding author.
Electronic address: aluru@uiuc.edu

[1] S. E. Lyshevski, *Fundamentals of Nano and Micro Engineering* (CRC Press, Boca Raton, FL, 2001); G. Yellen, Nature (London) **419**, 35 (2002); B. van der Bruggen, C. Vandecasteele, T. V. Gestel, W. Doyen, and R. Leysen, Environ. Prog. **22**, 46 (2003); A. Finkelstein, *Water Movement through Lipid Bilayers, Pores and Plasma Membranes* (Wiley, New York, 1987); S. A. Ben-Sasson and N. B. Grover, Adv. Physiol. Edu. **27**, 15 (2003).

[2] S. Murad and J. G. Powles, J. Chem. Phys. **99**, 7271 (1993); S. Murad, K. Oder, and J. Lin, Mol. Phys. **95**, 401 (1998); M. J. Kotelyanskii, N. J. Wagner, and M. E. Paulaitis, J. Membr. Sci. **139**, 1 (1998).

[3] A. Kalra, S. Garde, and G. Hummer, Proc. Natl. Acad. Sci. U.S.A. **100**, 10 175 (2003).

[4] T. Werder, J. H. Walther, R. L. Jaffe, T. Halicioglu, and P. Koumoutsakos, J. Phys. Chem. B **107**, 1345 (2003).

[5] S. Koneshan, J. C. Rasaiah, R. M. Lynden-Bell, and S. H. Lee, J. Phys. Chem. B **102**, 4193 (1998).

[6] P. G. Kusalik and I. M. Svishchev, Science **265**, 1219 (1994).

[7] E. Lindahl, B. Hess, and D. van der Spoel, J. Mol. Model. **7**, 306 (2001).

[8] T. Darden, D. York, and L. Pedersen, J. Chem. Phys. **98**, 10 089 (1993).

[9] R. Qiao and N. R. Aluru, J. Chem. Phys. **118**, 4692 (2003); Phys. Rev. Lett. **92**, 198301 (2004); R. Kjellander and H. Greberg, J. Electroanal. Chem. **450**, 233 (1998).